Configurational entropy calculations for refractory high-entropy alloys utilizing cluster expansion models: Supplementary Materials

Chiraag M Nataraj[1], Axel van de Walle*[1], and Amit Samanta†[2]

[1]School of Engineering, Brown University, Providence, RI 02912, USA
[2]Physics Division, Lawrence Livermore National Lab, Livermore, California 94550, USA

1 SRO Parameters

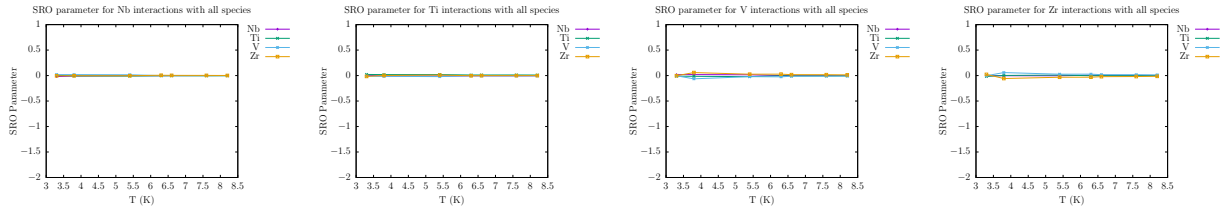

Figure 1: SRO parameters for NbTiVZr at 2500 K as a function of cut-off radius.

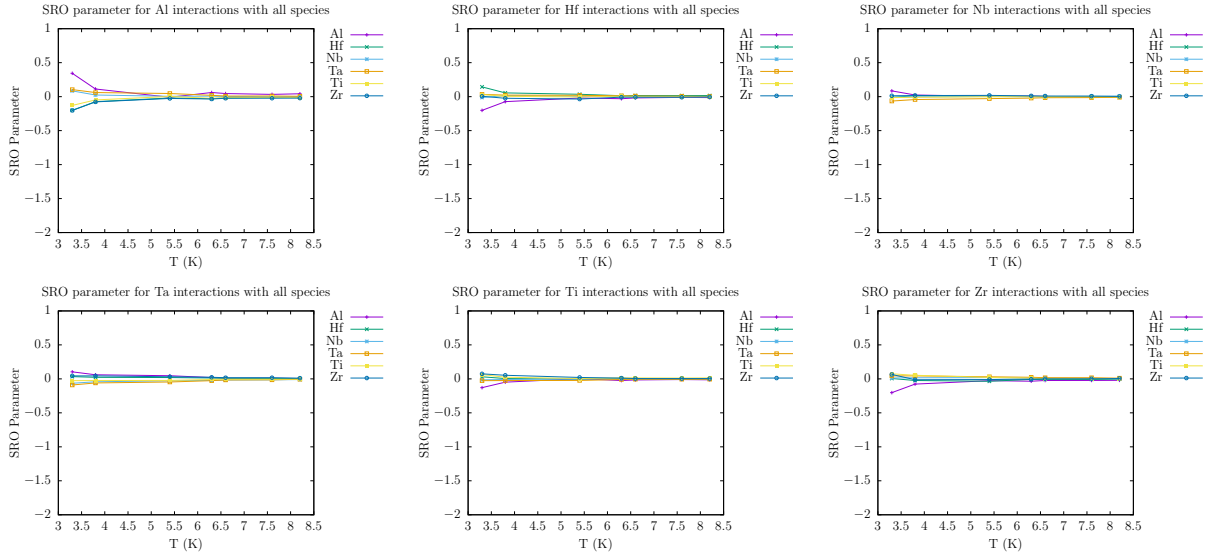

Figure 2: SRO parameters for AlHfNbTaTiZr at 2500 K as a function of cut-off radius.

2 MC results

*avdw@brown.edu
†samanta1@llnl.gov

	Number of samples					
	4000		12000		20000	
Temperature	$\langle E \rangle$	σ	$\langle E \rangle$	σ	$\langle E \rangle$	σ
250 K	-9088.63	1.26×10^{-3}	-9088.63	1.26×10^{-3}	-9088.63	1.27×10^{-3}
375 K	-9079.88	1.13×10^{-3}	-9083.35	5.73×10^{-4}	-9083.35	5.73×10^{-4}
500 K	-9071.95	4.65×10^{-4}	-9071.95	9.34×10^{-4}	-9071.94	1.53×10^{-3}
625 K	-9063.56	2.80×10^{-3}	-9063.74	7.27×10^{-3}	-9063.74	6.70×10^{-3}
750 K	-9056.67	1.91×10^{-2}	-9056.73	1.90×10^{-2}	-9056.77	1.71×10^{-2}
875 K	-9050.92	1.72×10^{-2}	-9051.24	4.54×10^{-2}	-9051.25	4.16×10^{-2}
1000 K	-9046.21	3.26×10^{-2}	-9046.25	4.07×10^{-2}	-9046.25	4.14×10^{-2}
1125 K	-9042.57	6.85×10^{-2}	-9042.43	9.95×10^{-2}	-9042.37	9.64×10^{-2}
1250 K	-9039.08	4.52×10^{-2}	-9039.11	5.28×10^{-2}	-9039.09	4.81×10^{-2}
1375 K	-9037.02	3.45×10^{-2}	-9037.00	2.65×10^{-2}	-9037.00	2.72×10^{-2}
1500 K	-9035.58	1.68×10^{-2}	-9035.58	1.83×10^{-2}	-9035.58	1.76×10^{-2}
1750 K	-9033.61	1.18×10^{-2}	-9033.61	1.19×10^{-2}	-9033.61	1.17×10^{-2}
2000 K	-9032.22	9.71×10^{-3}	-9032.23	1.02×10^{-2}	-9032.23	1.03×10^{-2}
2250 K	-9031.17	9.42×10^{-3}	-9031.17	9.37×10^{-3}	-9031.17	9.35×10^{-3}
2500 K	-9030.32	9.32×10^{-3}	-9030.32	9.20×10^{-3}	-9030.32	9.07×10^{-3}
2750 K	-9029.63	8.74×10^{-3}	-9029.63	8.96×10^{-3}	-9029.63	8.90×10^{-3}
3000 K	-9029.06	8.77×10^{-3}	-9029.06	8.84×10^{-3}	-9029.06	8.87×10^{-3}

Table 1: Mean ($\langle E \rangle$) and standard deviation (σ) of the total energy of the structure as the number of samples (structures) is increased (NbTiVZr).

	Number of samples					
	4000		12000		20000	
Temperature	$\langle E \rangle$	σ	$\langle E \rangle$	σ	$\langle E \rangle$	σ
100 K	-9849.12	1.24×10^{-4}	-9863.75	1.88×10^{-4}	-9863.75	1.88×10^{-4}
200 K	-9863.90	4.86×10^{-4}	-9863.90	4.86×10^{-4}	-9863.90	4.86×10^{-4}
300 K	-9863.24	5.64×10^{-4}	-9865.92	6.69×10^{-5}	-9865.92	6.69×10^{-5}
400 K	-9864.64	9.06×10^{-4}	-9869.40	2.57×10^{-3}	-9869.40	2.57×10^{-3}
500 K	-9866.34	1.53×10^{-3}	-9868.44	5.06×10^{-3}	-9868.44	5.06×10^{-3}
600 K	-9846.15	1.19×10^{-3}	-9864.90	7.80×10^{-3}	-9867.21	9.71×10^{-4}
700 K	-9863.29	6.18×10^{-3}	-9863.29	6.18×10^{-3}	-9865.57	5.25×10^{-3}
800 K	-9861.46	1.08×10^{-2}	-9861.44	1.52×10^{-2}	-9861.45	9.12×10^{-3}
900 K	-9861.36	8.56×10^{-3}	-9861.77	1.27×10^{-2}	-9862.66	1.22×10^{-2}
1000 K	-9860.48	1.39×10^{-2}	-9860.55	1.57×10^{-2}	-9860.55	1.60×10^{-2}
1100 K	-9854.42	1.19×10^{-2}	-9857.08	6.28×10^{-3}	-9857.10	2.00×10^{-2}
1200 K	-9854.20	1.20×10^{-2}	-9854.98	8.80×10^{-3}	-9855.22	8.28×10^{-3}
1300 K	-9850.93	1.34×10^{-2}	-9851.25	2.44×10^{-2}	-9851.64	2.24×10^{-2}
1400 K	-9847.99	2.52×10^{-2}	-9848.24	1.64×10^{-2}	-9848.23	1.75×10^{-2}
1500 K	-9844.26	7.44×10^{-3}	-9844.25	1.19×10^{-2}	-9844.24	1.75×10^{-2}
1600 K	-9838.79	1.80×10^{-2}	-9839.67	1.35×10^{-2}	-9839.67	1.61×10^{-2}
1700 K	-9833.29	2.00×10^{-2}	-9833.77	3.82×10^{-2}	-9834.33	3.65×10^{-2}
1800 K	-9827.47	8.11×10^{-3}	-9828.63	1.22×10^{-2}	-9829.23	1.31×10^{-2}
1900 K	-9821.45	4.70×10^{-4}	-9821.43	1.39×10^{-2}	-9821.41	2.30×10^{-2}
2000 K	-9813.19	2.98×10^{-2}	-9813.86	1.80×10^{-2}	-9813.83	2.78×10^{-2}
2100 K	-9804.49	5.19×10^{-2}	-9805.85	4.39×10^{-2}	-9807.28	2.15×10^{-2}
2200 K	-9797.94	1.56×10^{-2}	-9798.82	2.27×10^{-2}	-9798.84	1.98×10^{-2}
2300 K	-9791.08	1.73×10^{-2}	-9791.01	3.55×10^{-2}	-9791.00	5.09×10^{-2}
2400 K	-9782.74	5.75×10^{-2}	-9783.37	1.21×10^{-1}	-9783.39	9.96×10^{-2}
2500 K	-9775.51	6.12×10^{-2}	-9776.12	1.04×10^{-1}	-9776.58	8.08×10^{-2}
2600 K	-9767.92	8.05×10^{-2}	-9768.32	1.31×10^{-1}	-9768.37	1.19×10^{-1}
2700 K	-9760.95	9.92×10^{-3}	-9760.90	6.51×10^{-2}	-9760.79	8.32×10^{-2}
2800 K	-9751.61	5.83×10^{-2}	-9752.07	1.19×10^{-1}	-9751.98	1.56×10^{-1}
2900 K	-9742.54	6.68×10^{-2}	-9742.50	9.49×10^{-2}	-9742.61	1.38×10^{-1}
3000 K	-9733.32	9.04×10^{-2}	-9733.56	7.75×10^{-2}	-9733.57	7.87×10^{-2}

Table 2: Mean ($\langle E \rangle$) and standard deviation (σ) of the total energy of the structure as the number of samples (structures) is increased (HfNbTaTiZr).

	Number of samples					
	4000		12000		20000	
Temperature	$\langle E \rangle$	σ	$\langle E \rangle$	σ	$\langle E \rangle$	σ
250 K	-3780.42	3.49×10^{-4}	-3780.50	1.65×10^{-3}	-3780.50	2.07×10^{-3}
375 K	-3779.11	1.11×10^{-3}	-3779.11	1.67×10^{-3}	-3779.16	2.85×10^{-3}
500 K	-3774.65	1.23×10^{-3}	-3775.61	5.60×10^{-6}	-3775.61	5.74×10^{-6}
625 K	-3769.56	4.73×10^{-3}	-3769.55	4.33×10^{-3}	-3769.55	4.70×10^{-3}
750 K	-3764.06	1.11×10^{-2}	-3764.36	1.34×10^{-2}	-3764.33	1.90×10^{-2}
875 K	-3761.27	4.32×10^{-2}	-3761.33	5.22×10^{-2}	-3761.29	4.84×10^{-2}
1000 K	-3759.07	2.40×10^{-2}	-3759.11	3.00×10^{-2}	-3759.10	2.92×10^{-2}
1125 K	-3757.49	1.97×10^{-2}	-3757.49	2.15×10^{-2}	-3757.50	2.45×10^{-2}
1250 K	-3756.16	2.19×10^{-2}	-3756.15	2.24×10^{-2}	-3756.16	2.22×10^{-2}
1375 K	-3754.89	2.55×10^{-2}	-3754.90	2.74×10^{-2}	-3754.90	2.69×10^{-2}
1500 K	-3753.63	3.54×10^{-2}	-3753.65	3.84×10^{-2}	-3753.65	3.84×10^{-2}
1750 K	-3750.89	7.94×10^{-2}	-3750.91	9.55×10^{-2}	-3750.91	9.14×10^{-2}
2000 K	-3747.61	9.89×10^{-2}	-3747.76	2.14×10^{-1}	-3747.71	1.75×10^{-1}
2250 K	-3745.36	6.16×10^{-2}	-3745.35	5.40×10^{-2}	-3745.35	5.35×10^{-2}
2500 K	-3744.13	2.12×10^{-2}	-3744.13	2.25×10^{-2}	-3744.14	2.33×10^{-2}
2750 K	-3743.35	1.59×10^{-2}	-3743.34	1.55×10^{-2}	-3743.34	1.55×10^{-2}
3000 K	-3742.76	1.31×10^{-2}	-3742.75	1.24×10^{-2}	-3742.75	1.23×10^{-2}

Table 3: Mean ($\langle E \rangle$) and standard deviation (σ) of the total energy of the structure as the number of samples (structures) is increased (AlHfNbTaTiZr).

3 Phase Stability

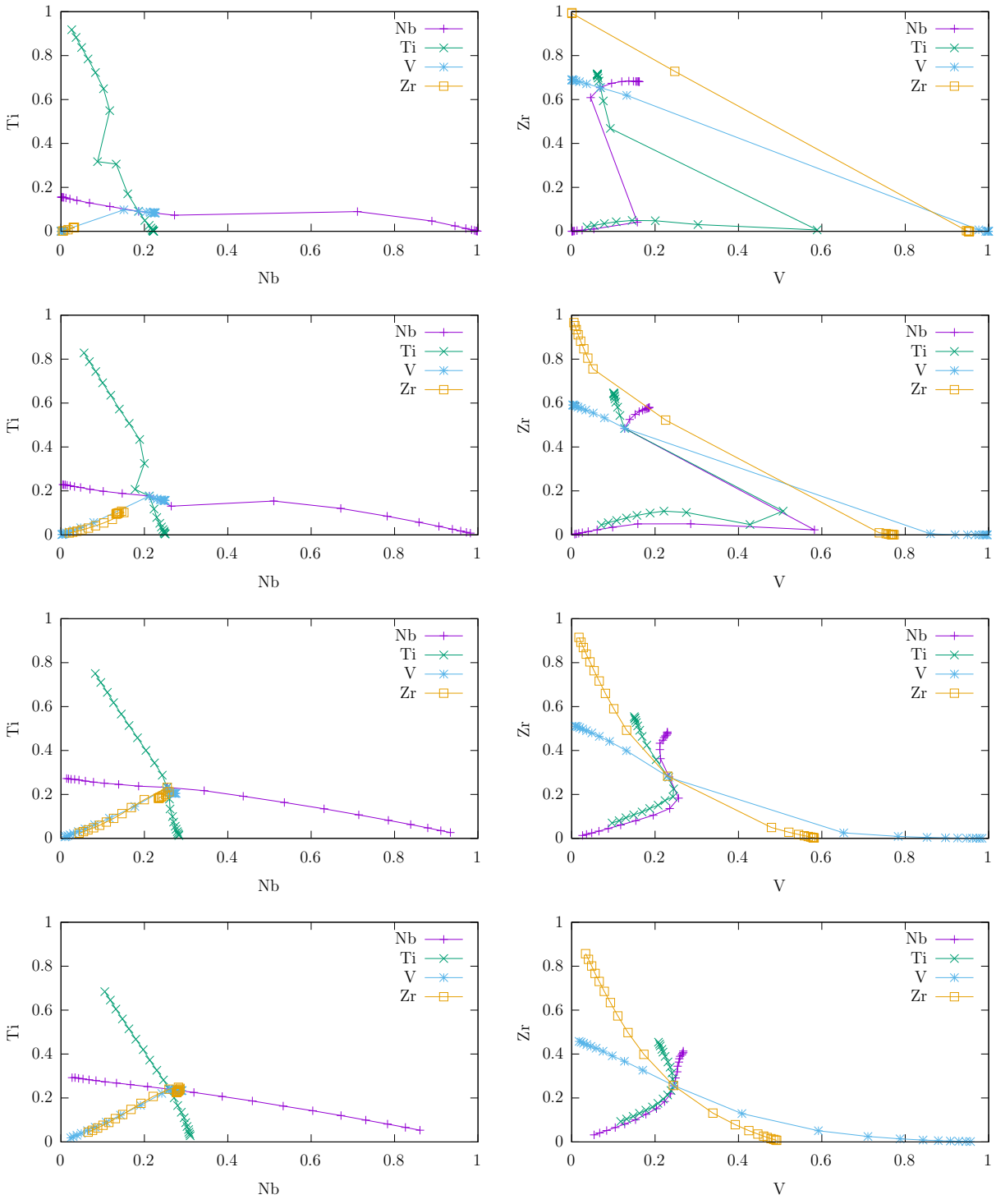

Figure 3: Results from Grand Canonical Monte Carlo simulations for NbTiVZr at various temperatures by row: 1000 K (top row), 1500 K, 2000 K, and 2500 K (bottom). Each curve tracks how concentrations of the various elements vary as the chemical potential of each species is varied independently. Jumps in concentrations signify a phase transition. These show the following phase changes: $\approx NbTiV_2$ to an equiatomic phase at 2000 K while varying the chemical potential of Zr, a roughly equiatomic phase to a Nb-Ti-V rich phase at 2000 K while varying the chemical potential of V, a V-rich Nb-Ti-V phase to a Zr-rich phase containing all four elements at 1500 K while varying the chemical potential of Zr, a Zr-rich phase containing all four elements to a V-rich Nb-Ti-V phase at 1500 K while varying the chemical potential of V, a Zr-rich phase containing all four elements to a V-rich phase containing all four elements at 1500 K while varying the chemical potential of Ti, and a Zr-rich phase containing all four elements to a V-rich Nb-Ti-V phase at 1500 K while varying the chemical potential of Nb.

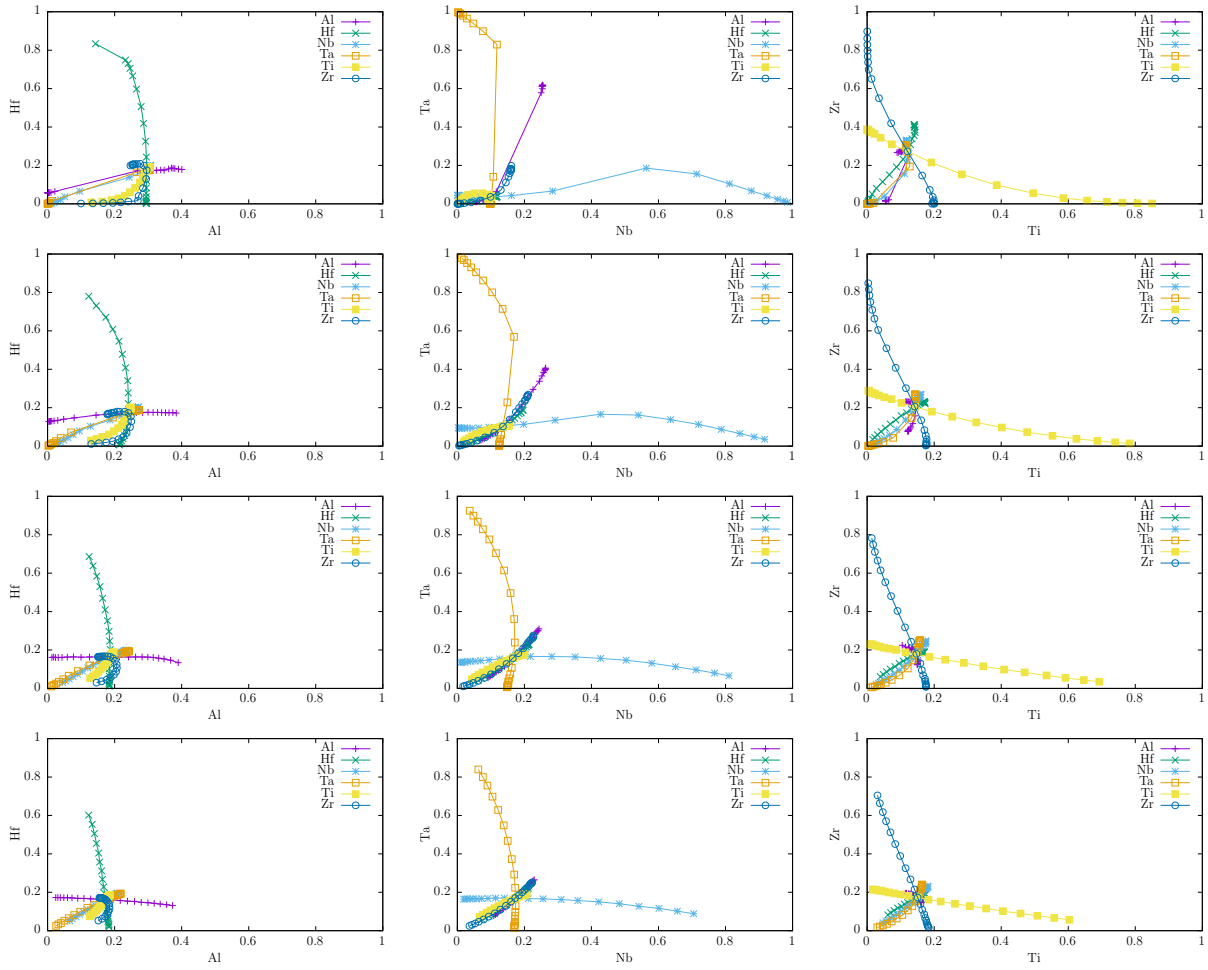

Figure 4: Results from Grand Canonical Monte Carlo simulations for AlHfNbTaTiZr at various temperatures by row: 1000 K (top row), 1500 K, 2000 K, and 2500 K (bottom). Each curve tracks how concentrations of the various elements vary as the chemical potential of each species is varied independently. Jumps in concentrations signify a phase transition. These show the following phase changes: a roughly equiatomic phase to a Ta-rich phase at 1500 K while varying the chemical potential of Ta, and a roughly equiatomic phase to a Nb-Ta-rich phase at 1500 K while varying the chemical potential of Nb.